BER Comparison Between Time-Domain and Frequency-Domain Self-Interference Canceller in 5G-Based Full-Duplex Mobile Communications

Takumi Yasaka†, Kazuma Matsushima†, Satoshi Suyama‡, and Hiroyuki Otsuka†

†Graduate School of Engineering, Kogakuin University, 1-24-2, Shinjuku-ku, Tokyo, 163-8677 Japan
‡6G-Tech Department, NTT DOCOMO, INC. 3-5 Hikarinooka, Yokosuka-shi, Kanagawa, 239-8536 Japan
e-mail: cm23069@ns.kogakuin.ac.jp

***Abstract*—Full-duplex mobile communications are gaining attention as an access method between base station (BS) and user equipment (UE) that can improve frequency utilization efficiency. The important technology is to cancel or eliminate self-interference that occurs between the transmitter (TX) and its own receiver (RX) at both BS and UE. This paper presents a BER comparison between time-domain and frequency-domain self-interference canceller (SIC) operated at baseband. Specifically, we show the BER performance of OFDM-based QPSK and 16/64/256/1024-QAM signals as parameters of the coding rate when time-domain or frequency-domain SIC is applied. The results indicate that both SIC can drastically improve the BER for QPSK and QAM signals compared without SIC, and the frequency-domain SIC is more effective as the modulation order of QAM increases.**

Keywords—mobile communication, full-duplex, self-interference canceller, OFDM, 1024-QAM

I. Introduction

Most fifth-generation (5G) mobile systems use time division duplex (TDD) communication on the same carrier frequency band. This approach enables more efficient spectrum utilization, particularly when upload and download traffic demands are uneven. In contrast, fourth-generation (4G) mobile systems predominantly use frequency division duplex (FDD) communication globally. FDD relies on separate frequency bands for uplink and downlink, allowing data to be transmitted in both directions simultaneously. However, neither TDD nor FDD can achieve perfectly simultaneous two-way communication without incorporating some form of time-switching or frequency separation [1]–[3].

Full-duplex mobile communication has garnered significant attention due to its ability to transmit and receive simultaneously on the same frequency band, outperforming both TDD and FDD systems. This technology effectively doubles spectral efficiency by allowing the same frequency resources to be used for both uplink and downlink at the same time. However, the primary challenge in full-duplex communication is self-interference. This occurs when the downlink signal transmitted by the base station (BS) interferes with the uplink signal received at the BS. Similarly, self-interference can also happen between the transmitter (TX) and its own receiver (RX) within the user equipment (UE).

In the past, full-duplex wireless communication was studied, but it was considered impractical due to significant self-interference [4]. In 2010, a technical paper suggesting the possibility of full-duplex wireless transceiver has been presented, which proposed a novel technique for self-interference cancellation [5]. Since then, many research findings have been published [6]–[17]. In [6], novel analog and digital cancellation techniques that cancel the self-interference to the receiver noise floor under the condition of Wi-Fi 802.11ac PHY. In [8], full-duplex MAC protocol for multi-hop network was proposed to achieve a higher throughput than conventional such as CSMA/CA. In [10], potential techniques including passive suppression, analog cancellation, and active digital cancellation were introduced. In [7], [15], full-duplex relay which the backhaul and access links simultaneously operate on the same carrier frequency was discussed. In [18], [19], digital self-interference canceller (SIC) based on 5G-based orthogonal frequency division multiplexing (OFDM) was proposed in which a demodulation reference signal (DMRS) arrangement enables the highly channel estimation of self-interference. In [20]–[22], we presented the transmission performance of OFDM-based 1024- quadrature amplitude modulation (QAM) signals, when applying frequency-domain SIC using DMRS. Until now, there has not been sufficient comparison of the characteristics between time-domain SIC and frequency-domain SIC in the baseband. In particular, the performance evaluation for higher-order QAM has been insufficient.

In this paper, we present the bit error rate (BER) performance of OFDM-based quadrature phase shift keying (QPSK) and QAM signals as a function of coding rates. We consider scenarios where time-domain or frequency-domain SIC is applied at the baseband in full-duplex mobile communication. Specifically, the BER values are evaluated using 5G system parameters under a static self-interference channel response. Section II outlines the configurations for frequency-domain SIC using DMRS and time-domain SIC. In Section III, we describe two types of simulation block diagrams: one for frequency-domain SIC and the other for time-domain SIC. Finally, Section IV provides the conclusions of our study. Furthermore, future research topics will also be addressed in Section IV.

II. Self-Interference Canceller

Figure 1 illustrates full-duplex mobile communication system between a BS and a single UE, where uplink and downlink transmissions occur simultaneously (t_1) on the same carrier frequency (f_1). When the BS transmits a downlink signal, it interferes with the uplink signal received by the BS's RX. These interactions between the TX and its own receiver RX are known as self-interference. Therefore, to enable full-duplex mobile communication, effectively mitigating or canceling self-interference is crucial.

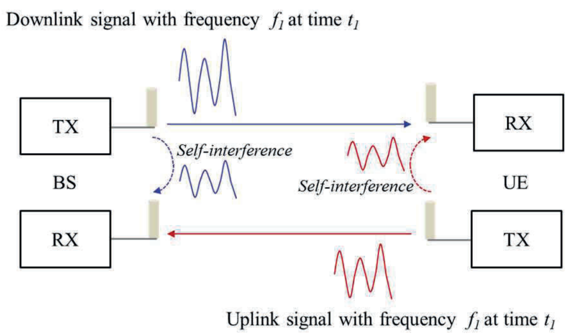

Fig. 1. Full-duplex mobile communication between BS and UE.

A. Frequency-domain SIC

The DMRS is used to support channel estimation between the BS and UE, as well as data demodulation. It helps the receiver accurately assess the impact of the wireless channel, including effects like multipath fading [2]. In this paper, frequency-domain SIC leverages DMRS for self-interference channel estimation. Figure 2 illustrates the architecture of a baseband frequency-domain SIC system at the BS utilizing downlink DMRS. The downlink transmission signal, which includes the blue-colored DMRS, interferes as self-interference with the uplink signal received from the UE at the BS's RX. The self-interference channel between the BS TX and its receiver RX can be estimated by correlating the known transmitted blue-colored DMRS with the received DMRS in the self-interference signal. The transmit data signals are then adjusted using a weighting vector (comprising phase and amplitude) derived from this correlation through a linear interpolation process. In other words, a replica of the self-interference signal can be generated sequentially from the viewpoints of frequency-domain. By subtracting this replica from the received uplink signal, self-interference can be effectively removed.

In this scenario, the downlink DMRS mapping must be shifted relative to the uplink DMRS mapping in the frequency domain to prevent overlap. In this way, the mapping positions of the DMRS for the downlink and uplink are shifted in frequency, which reduces the number of OFDM symbols allocated for data. As a result, the data rates are slightly lower compared to FDD or TDD.

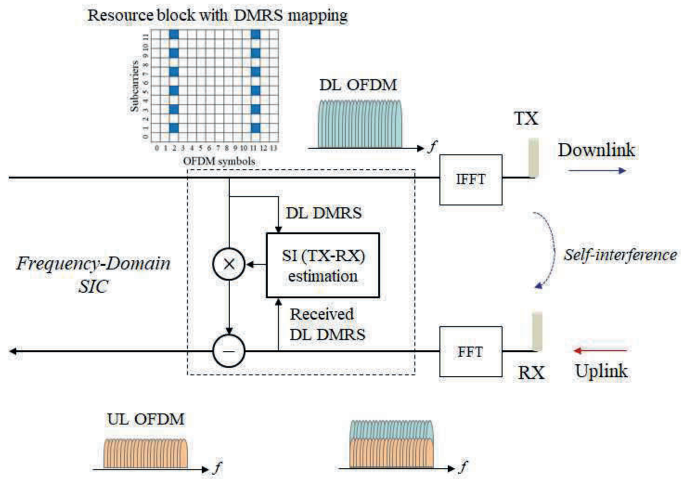

Fig. 2. Configuration of baseband frequency-domain SIC.

B. Time-domain SIC

Figure 3 shows the configuration of baseband time-domain SIC. The self-interference channel estimation can be performed by the correlation detection directly between the known transmit data signal and the received the data signal. Therefore, the time-domain SIC do not use DMRS for estimating the self-interference channel unlike frequency-domain SIC. The cancellation process of time-domain-SIC is almost the same as that of frequency-domain SIC. TX data signals are adjusted using weighting vector obtained by the correlation detection. Then, by subtracting the time-domain replica from the received uplink signal, the self-interference can be eliminated. After processing FFT, the desired uplink signal is demodulated by using uplink DMRS.

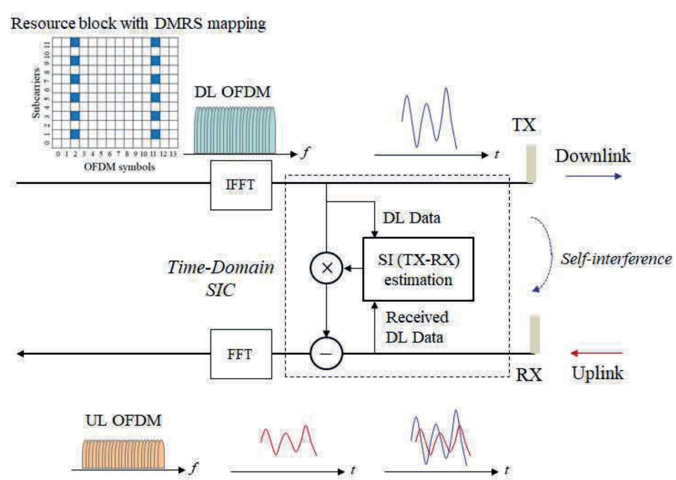

Fig. 3. Configuration of baseband time-domain SIC.

III. Simulation Conditions and Results

A. Simulation parameters and block diagrams

Table I shows the main simulation parameters. The bandwidth of OFDM signal is 100 MHz in which the subcarrier spacing is 30 kHz. Low-density parity-check (LDPC) codes are employed for error correction purposes in the encoder. LDPC is used for data channel PDSCH (Physical data shared channel) in 5G that provides the performance close to Shannon limit. BER is evaluated over 1,000 slots, with each slot containing 14 OFDM symbols. The desired-to-undesired signal ratio (DUR) at the BS RX is defined as the ratio between the desired uplink signal power and the self-interference power.

TABLE I. Primary Simulation Parameters

Parameter	Value
Encoder	LDPC
Symbol modulation	QPSK, 16/64/256/1024-QAM
OFDM bandwidth	100 MHz
OFDM subcarrier spacing	30 kHz
FFT size	4096
Sampling rate	122.88 MHz
Number of transmission slots	1,000, (14 OFDM symbols/slot)
Cyclic prefix length	2380 ns

Figure 4 shows a simulation block diagram of frequency-domain SIC, where the configuration of UE TX is same as that of BS TX. DUR is varied using a gain adjustment (Gain adj.). The frequency-domain SIC operates in the region before IFFT process in BS TX and after FFT process in BS RX.

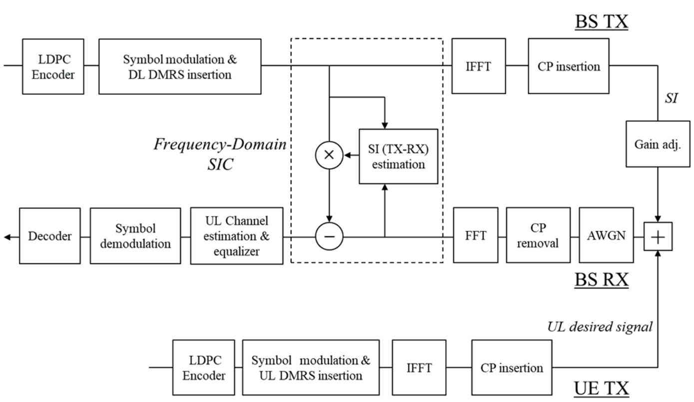

Fig. 4. Simulation block diagram equipped with frequency-domain SIC.

Figure 5 shows a simulation block diagram of time-domain SIC, which operates in the region after IFFT process in BS TX and before FFT process in BS RX. Both simulation block diagrams as shown in Figs. 4 and 5 are created using MATLAB/Simulink.

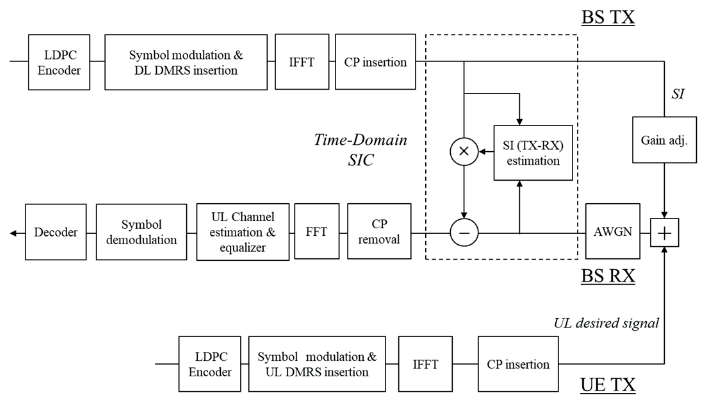

Fig. 5. Simulation block diagram equipped with time-domain SIC.

B. BER performance

Modulation and coding scheme (MCS) refers to the combination of modulation method and coding rate. In this paper, we consider 32 different types of MCS indexes [23], with the maximum modulation method is 1024-QAM. We examine the BER as a function of the received signal-to-noise ratio (SNR) for five types of MCS, using either frequency-domain SIC or time-domain SIC under two different DUR conditions of −30 dB and −60 dB.

Figure 6 shows BER when using frequency-domain SIC at a DUR of −30 dB. Here, the green, blue, purple, red, and yellow lines indicate the BERs for using MCS 4 (QPSK, coding rate (CR)≈ 0.6), MCS 10 (16-QAM, CR≈ 0.64), MCS 19 (64-QAM, CR≈ 0.85), MCS27 (256-QAM, CR≈ 0.92), and MCS 31 (1024-QAM, CR≈ 0.91), respectively. The black line represents the BER without SIC, i.e., SIC OFF. Figure 7 shows BER when using time-domain SIC at a DUR of −30 dB. Both SIC are much effective to eliminate self-interference. BERs for using MCS 4, MCS 10, and MCS 19 are not so different between the use of frequency-domain SIC and time-domain SIC. If we had to choose, when the modulation order is low, the BER when using time-domain SIC is slightly better than that when using frequency-domain SIC. However, as the modulation order increases, the BER when using time-domain SIC degrades if the coding rate remain unchanged. For example, BERs for MCS 27 and MCS 31 when using time-domain SIC worse than those when using frequency-domain SIC.

Figure 8 shows BER when using frequency-domain SIC at a DUR of −60 dB. Figure 9 shows BER when using time-domain SIC at a DUR of −60 dB. Similar to previous results, BERs for MCS 27 and MCS 31 when using time-domain SIC worse than those when using frequency-domain SIC, however both SIC are effective to eliminate self-interference. We consider it’s because the reason is likely due to the estimation accuracy and the control response due to the correlation detection. Figure 10 shows BERs for 256- and 1024-QAM as a function of the coding rate. As the coding rate reduces, the BER improves. In this way, LDPC codes are also effective for signal detection due to the error associate with self-interference.

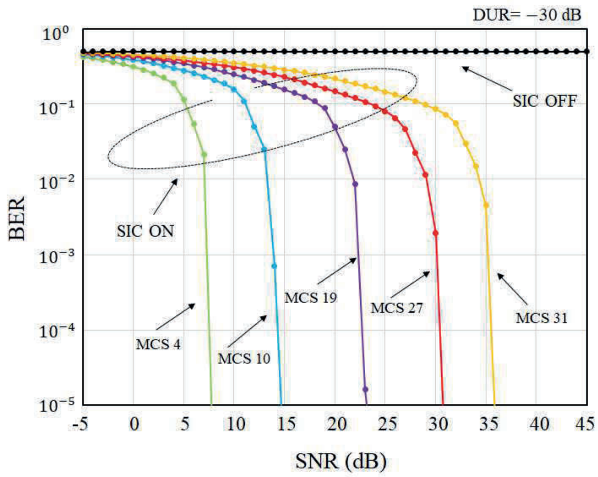

Fig. 6. BER when using frequency-domain SIC at DUR of −30 dB.

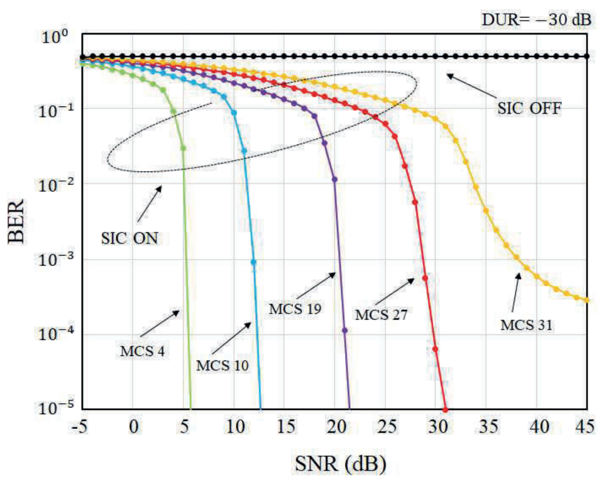

Fig. 7. BER when using time-domain SIC at DUR of −30 dB.

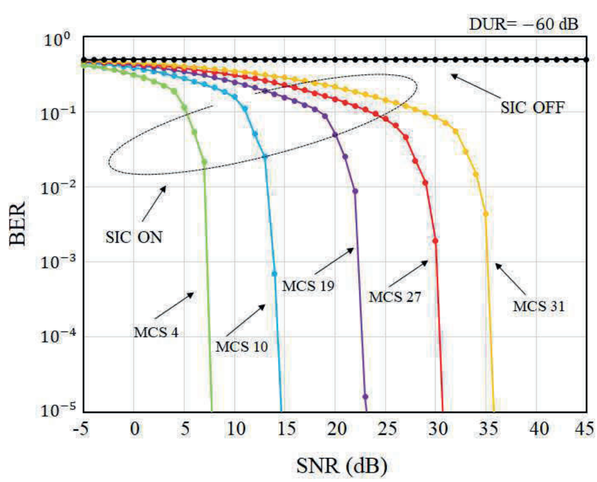

Fig. 8. BER when using frequency-domain SIC at DUR of −60 dB.

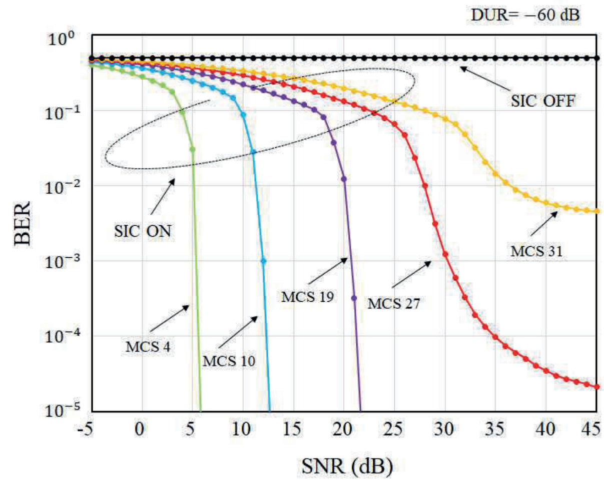

Fig. 9. BER when using time-domain SIC at DUR of −60 dB.

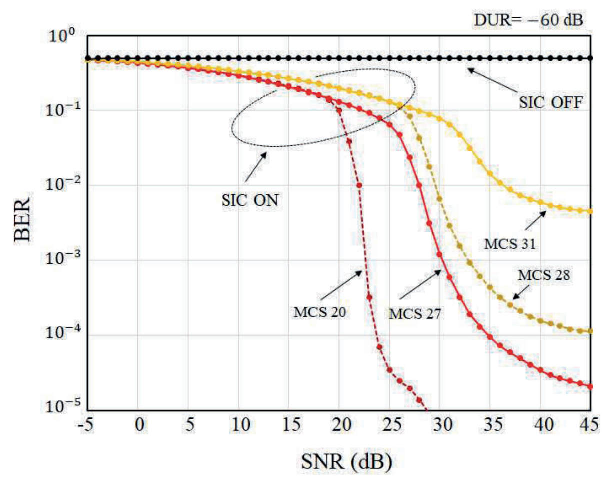

Fig. 10. BER for 256- and 1024-QAM as a function of the coding rate when using time-domain SIC at DUR of −60 dB.

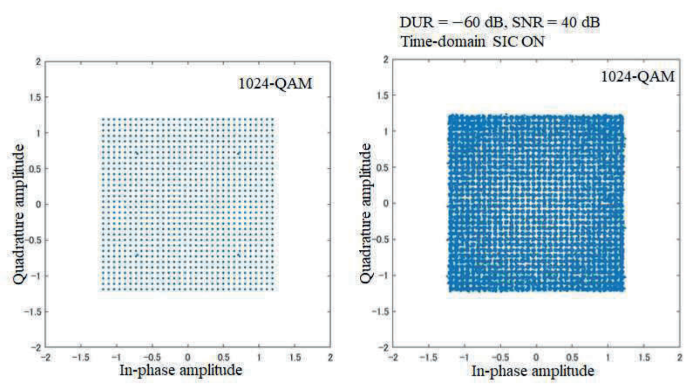

(a) Transmitter side (UE TX)

(c) Receiver side (BS RX)

Fig. 11. Signal constellations of 1024-QAM at DUR of −60 dB when using time-domain SIC.

Figure 11 shows photos of 1024-QAM signal constellations observed at transmitter side (UE TX) and the receiver side (BS RX) when using time-domain SIC, respectively, at a DUR of −60 dB and an SNR of 40 dB. The signal constellation at the receiver side slightly worsens compared with that at transmitter side, because the time-domain SIC cannot eliminate the self-interference perfectly.

IV. Conclusion

This paper presented a BER comparison between time-domain self-interference canceller (SIC) and frequency-domain SIC operated at baseband in full-duplex mobile communications. Specifically, we demonstrated the BER of OFDM-based QPSK and 16/64/256/1024-QAM signals as a function of the coding rate using 5G system parameters when using time-domain or frequency-domain SIC. It was confirmed that both SIC can drastically improve the BER compared without SIC. Furthermore, when the modulation order was low, the BER when using time-domain SIC was slightly better than that when using frequency-domain SIC. However, as the modulation order of QAM increased, the BER when using time-domain SIC degraded if the coding rate remained unchanged, i.e., the frequency-domain SIC was more effective as the modulation order increased. This report evaluates the performance of SIC under the conditions that there is no fading between the transmitting (BS TX) and receiving (BS RX) antennas.

In our future research, we will evaluate the performance of SIC in environments where self-interference varies over time, such as under fading conditions. Especially for frequency-domain SIC, we clarify the optimal the number of DMRS to meet the requirements under fading conditions.

Acknowledgment

This work was supported in part by JSPS KAKENHI Grant Number JP21K11874, Grant-in-Aid for Scientific Research (C).

References

[1] D. Soldani and A. Manzalini, “Horizon 2020 and beyond; On the 5G operating system for a truly digital society,” *IEEE Veh. Tech. Mag.*, vol. 10, no. 1, pp. 32-42, March 2015.

[2] 3GPP TR 23.501, “System architecture for the 5G system (5GS),” Release 15, June 2018.

[3] K. Balachandran, J. H. Kang, K. Karakayali, and K. M. Rege, “Flexible duplex in FDD spectrum,” in *Proc. ICC workshops*, pp. 1-6, May 2017.

[4] A. Goldsmith, Wireless Communications, *Cambridge University Press*, 2005.

[5] J.I. Choi, M. Jain, K. Srinivasan, P. Levis, and S. Katti, “Achieving single channel, full duplex wireless communication,” in *Proc. 16th ACM MobiCom’10*, pp.1–14, Sept. 2010.

[6] D. Bharadia, E. Mcmilin, and S. Katti, “Full duplex radios,” *ACM Sigcomm Computer Commun. review*, vol. 43, no.4, pp.375-386, Oct. 2013.

[7] Y. Bo, L. Yang, X. Cheng, and R. Cao, “Transmit power optimization for full duplex decode-and-forward relaying,” in *Proc. Globecom2013*, pp. 3347-3352, Dec. 2013.

[8] K. Tamaki, Y. Sugiyama, A. Raptino, M. Bandai, S. Saruwatari, and T. Watanabe, “Full duplex media access control for wireless multi-hop networks,” in *Proc. VTC2013-Spring*, pp.1–6, June 2013.

[9] A. Sabharwal, P. Schniter, D. Guo, D.W. Bliss, S. Rangarajan, and R. Wichman, “In-band full-duplex wireless: Challenges and opportunities (invited paper),” *IEEE J. on Selected Areas in Commun.*, vol. 32, no. 9, pp.1637-1652, Sept. 2014.

[10] Z. Zhang, X. Chai, K. Long, A. V. Vasilakos, and L. Hanzo, “Full duplex techniques for 5G networks: self-interference cancellation, protocol design, and relay selection,” *IEEE Commun. Magazine*, vol. 53, no. 5, pp. 128-137, May 2015.

[11] J. Zhou, T.H. Hao, T. Dinc, and H. Krishnaswamy, “Integrated Wideband Self-Interference Cancellation in the RF Domain for FDD and Full-Duplex Wireless,” *IEEE J. of Solid-State Circuits*, vol. 50, no. 12, pp. 3015-3031, Dec. 2015.

[12] R. Keating, R. Ratasuk, and A. Ghosh, “Performance analysis of full duplex in cellular systems,” in *Proc. VTC2016-Spring*, pp. 1-5, May 2016.

[13] Z. Zhang, K. Long, A. V. Vasilakos, and L. Hanzo, “Full-Duplex Wireless Communications: Challenges, Solutions, and Future Research Directions,” *Proc. of the IEEE*, vol. 104, issue 7, pp. 1369-1409, July 2016.

[14] U. Siddique, H. Tabassum, and E. Hossain, “Downlink spectrum allocation for in-band and out-band wireless backhauling of full-duplex small cells,” *IEEE Trans. on Commun.*, vol. 65, no. 8, pp. 3538-3554, April 2017.

[15] H. Utatsu and H. Otsuka, “Performance analysis of fiber-optic relaying with simultaneous transmission and reception on the same carrier frequency,” *IEICE Trans. Commun.*, vol. E102-B, no. 8, pp.1771-1780, August 2019.

[16] W. Wang and Z. Zhang, “DBF Based Channel Estimation for Self-interference Cancellation in Full-Duplex Communications,” in *Proc. ICCCS2021*, pp. 564-569, April 2021.

[17] A. Nagulu, N. Reiskarimian, T. Chen, S. Garikapati, I. Kadota, and T. Dinc, “Doubling Down on Wireless Capacity: A Review of Integrated Circuits, Systems, and Networks for Full Duplex,” *Proc. of the IEEE*, vol. 112, issue 5, pp. 405-432, May 2024.

[18] S. Mori, K. Mizutani and H. Harada, "Digital Self-Interference Cancellation for 5G-baesd Full Duplex Cellular System", in *Proc. PIMRC2022*, pp. 1165-1170, Sept. 2022.

[19] H. Harada, K. Mizutani, T. Matsumura, T. Kato, and K. Shioiri, “Development of Full-Duplex Cellular System for Beyond 5G and 6G Systems,” in *Proc. PIMRC2022*, pp. 1-5, Sept. 2022.

[20] T. Yasaka, T. Yamada, S. Suyama, and H. Otsuka, “Proposal of Self-Interference Canceller Using DMRS for Full Duplex Mobile Communications,” in *Proc. VTC2023-Spring*, W9-8, pp. 1-5, June 2023.

[21] T. Yasaka, K. Matsushima, F. Hatsuki, S. Suyama, and H. Otsuka, “Performance of Self-Interference Canceller in SDR-Based Full-Duplex System,” in *Proc. ICOIN2024*, pp. 340-344, Jan. 2024.

[22] K. Matsushima, T. Yasaka, and H. Otsuka, “Consideration of Frequency Domain Adaptive SIC for Full-Duplex Communication,” in *Proc. ICUFN2024*, pp. 1-5, August 2024.

[23] N. Inagaki and H. Otsuka, “Design Flexibility of Picocells in HetNets with Respect to Number of Picocell-Sectors,” in *Proc. ICUFN2024*, pp. 1-5, August 2024.